CONF-791018--2

AN EXPERIMENTAL STUDY OF VIRTUAL IMPACTORS

by

Thomas J. Yule and Christopher G. Broniarck

MASTER

Prepared for

Second Symposium

on

Advanced in Particle Sampling and Measurement

Daytona, Florida

October 7-10, 1979

U of C-AUA-USDOE

ARGONNE NATIONAL LABORATORY, ARGONNE, ILLINOIS

Operated under Contract W-31-109-Eng-38 for the

U. S. DEPARTMENT OF ENERGY

AN EXPERIMENTAL STUDY OF VIRTUAL IMPACTORS*

Thomas J. Yule
Argonne National Laboratory

and

Christopher G. Broniarck
Rensselaer Polytechnic Institute

ABSTRACT

Virtual impactors are currently being used in a number of instruments to separate an aerosol into different size ranges. The virtual impactor is a variation of the standard impactor in which the impaction surface is replaced by an orifice into which particles can pass and be collected or counted. We have made an experimental study of the collection characteristics of virtual impactors. The parameters varied included: acceleration nozzle-to-collection probe distance, the ratio of the collection probe-to-acceleration nozzle diameters, and the ratio of collection probe-to-inlet flows. Measurements were also made with different collection probe geometries. It was found that it is possible to parameterize much of the data by introduction of the Stokes number and an effective minor flow collection efficiency. One disadvantage of the virtual impactor is that in the transition region particles are collected on the inside walls of the collection probe near the probe tip. The amount that is collected is a sensitive function of the probe geometry.

*Research performed under the auspices of the U. S. Department of Energy.

AN EXPERIMENTAL STUDY OF VIRTUAL IMPACTORS

INTRODUCTION

Virtual impactors are currently being used in a number of instruments to separate an aerosol into different size ranges. The virtual impactor is a variation of the standard impactor in which the impaction surface is replaced by a collection probe into which large particles will pass and then be collected or counted. Figure 1 is a schematic illustrating the operation of a virtual impactor. The aerosol stream is drawn through the acceleration nozzle where the velocity of the particles is increased. A collection probe is located at a short distance below the acceleration nozzle. Flow conditions are maintained such that the flow in the collection probe is a fixed fraction of the inlet flow. A few representative streamlines are shown on the figure.

In order to understand the principle of operation, consider particles that exit from the acceleration nozzle near streamlines which do not pass through the collection probe. Small particles follow the streamlines and remain in the flow that does not pass through the collection probe; large particles are unable to follow the streamlines in regions of rapidly changing curvature and become caught up in the flow that passes through the collection probe. The flow in the collection probe, Q_1, is referred to as the minor flow. The ratio Q_1/Q_0, where Q_0 is the inlet flow, ranges in value from 0.03 to 0.25 in present designs. For zero particle size a fraction of the particles equal to Q_1/Q_0 follow the streamlines of the minor flow and pass through the collection probe. The small particles that enter the collection probe along with the large particles introduce cross contamination. The flow which does not enter the collection probe is referred to as the major flow; it contains most of the small particles.

Virtual impactors possess a number of advantages over standard impactors. These are: the size and placement of the size-separated sample can be optimized for the analysis system, particle bounce and reentrainment are minimized, and significant amounts of a sample can be collected without serious loading problems and without change in collection efficiency. There are also disadvantages.

These are: the slope of the efficiency curve is less steep than that for a well-designed standard impactor, there is always some cross contamination, and some of the sample is collected on the inside walls of the collection probe.

The method of virtual impaction was introduced by Hounam and Sherwood[1] in 1965. They designed and constructed a multi-stage device called a cascade centripeter, which had cutpoints of 1.2, 3.5, and 12 micrometers. Flat orifice plates were used instead of acceleration nozzles. Their device had considerable wall losses. Shortly afterward, Conner[2] investigated the collection efficiency of a single-stage virtual impactor as a function of operating parameters.

More recently, interest in virtual impactors has been heightened by the U. S. Environmental Protection Agency's desire for a device which collects size-segregated ambient aerosol samples for large-scale monitoring applications. The device, which is referred to as a dichotomous sampler, separately collects fine (<2.5 micrometer) and coarse (>2.5 micrometer) airborne particles. An early design, which has two stages, is described by Dzubay and Stevens[3] and Loo, et al.[4] A second generation sampler, which has only a single stage and very low internal losses, has been developed by Loo, et al.[5] Virtual impactors have also appeared in other devices. McFarland, et al.[6] have developed a sampler that was used to collect large quantities of particulate matter from the stack of a coal-fired power plant. Kotrappa, et al.[7] and Yule[8] have used virtual impactors to size segregate radioactive aerosols in radiation detection instruments.

To aid in the development of the devices described above, various experimental studies on virtual impactors were undertaken. The most extensive studies are those by Loo, et al.[4] and by McFarland, et al.[9] Both studies were aimed at determining the optimum parameters for attaining sharp cutoffs with minimum internal losses for particular systems. The study reported here is somewhat broader in scope. It was undertaken to provide sufficient information to determine the cutoff size and collection characteristics for a wide range of system parameters. The study was patterned after the study on standard impactors by Marple and Liu.[10]

There have also been some theoretical studies of virtual impactors by Marple and Chien[11] and by Hassan, et al.[12] In general, these studies have given insight into the separation characteristics, but the agreement between measured and predicted data is not as good as that for the standard impactor.

EXPERIMENTAL METHODS

The collection characteristics of virtual impactors were studied using monodisperse aerosols. Most of the measurements were made with dioctyl phthalate (DOP) droplets, which contained trace amounts of uranine (the sodium salt of fluorescein) dye as a tracer. Aerosols with sizes from 1 to 10 micrometers were generated with a Berglund-Liu vibrating-orifice aerosol generator. Some measurements were also made with polystyrene latex (PSL) aerosols. The PSL aerosol generator consisted of a nebulizer, diluter, diffusion dryer, and Kr-85 charge neutralizer. The collection characteristics for the two aerosols are expected to be different since one is a liquid droplet which will stick on contacting a surface, while the other is an elastic sphere which can rebound from a surface. The results obtained with the DOP aerosols represent an upper limit for collection on surfaces of the virtual impactor and are easier to compare with calculated results, because one can assume any droplet that comes in contact with a surface will stick to that surface.

Figure 2 is a schematic view of the single-stage virtual-impactor test assembly that was used for the measurements. The assembly allows one to easily change the acceleration nozzle and collection probe geometries. For measurements with the DOP aerosols the quality of the aerosols was monitored with an optical particle counter that had the probe located in a region above the inlet. A Bausch and Lomb 40-1A counter was used with a modified flow system, as described by Marple, et al.,[13] and with interface electronics that allows pulse-height analysis with a multichannel analyzer. Such a monitor is very useful in determining whether the aerosol generator is operating properly. For the measurements with DOP aerosols filters were inserted in the minor and major flow lines. Flow measurements were made with pressure-corrected rotameters. Measurement times were on the order of 15 minutes. The aerosol depositions were determined on various components: the underside of the piece supporting the acceleration nozzle, the acceleration nozzle, the collection probe, and the major and minor flow filters. These are the only areas where there are significant deposits. The deposits were determined by washing the pieces or filters in measured amounts of a buffer solution (0.05 M Na_2PO_4) and using fluorescence techniques. A Turner Model 110 fluorometer was used; calibration curves had been determined which relate the absorption to the uranine concentration. Concentrations as low as 0.005 μg/ml can be reliably determined.

For measurements with the PSL aerosols two aerosol sizes were used: 1.10 and 2.02 micrometer. The optical particle counter probe was placed in a region below the collection probe. For these measurements only the fraction of the incoming aerosol that passed through the collection probe was determined. For a given particle size and flow conditions, the aerosol concentrations before and after each measurement were determined by setting the major flow, Q_2, equal to zero and Q_0 equal to the nominal value of Q_1. The average concentration, $\overline{C}_{Q_2=0}$, was determined. With the nominal values of Q_0 and Q_2 established, the concentration, C, in the minor flow was measured. The minor flow collection efficiency, E_m, is simply

$$E_m = \frac{C}{(Q_0/Q_1)\ \overline{C}_{Q_2=0}} \ . \qquad (1)$$

RESULTS AND DISCUSSION

A series of measurements were made with DOP aerosols in which various geometrical and flow conditions were varied. A virtual impactor with geometrical and flow parameters listed in Table 1 was chosen as a standard; individual parameters were varied about these values. A value of D_1/D_0 = 1.28 was chosen for the standard, because this value results in minimum wall losses in the collection probe. The shape of the collection probe is the same as that shown in Figure 1. As is discussed below, this shape is not the optimum shape for minimum collection on the interior walls of the collection probe; however, it is a shape that has been used in a number of devices and is easy to treat analytically. Figure 3 shows the collection characteristics for the standard. Since the deposits in the acceleration nozzle and on the underside of the piece supporting the acceleration nozzle were very small, they are now shown. The minor flow collection efficiency is 0.25, which is simply the ratio Q_1/Q_0, for small particle sizes and reaches a value of 1.00 for large particle sizes. The region in which the minor flow collection efficiency is varying is referred to as the transition region. It is useful to define an effective minor flow collection efficiency, E_m',

$$E_m' = \frac{E_m - Q_1/Q_0}{1 - Q_1/Q_0} , \qquad (2)$$

which corresponds to the efficiency for removing particles from the major flow and having them pass through the collection probe. E_m' may assume values from zero to unity. We choose to define the cutoff for a virtual impactor as that size for which $E_m' = 0.5$. Note that is is only in the transition region that there is significant collection on the walls of the collection probe. For the standard the maximum value is approximately 0.20. For aerosols that have a probability of rebounding from contact with a wall, this maximum is reduced. In order to investigate the wall losses in the collection probe in more detail, a special collection probe, shown in Figure 4, was constructed. The thickness of the annular inserts was one-third D_0. Measurements were made with 2, 2.5, and 3 micrometer DOP aerosols. For all sizes close to 100% of the deposit appeared on the inside of the top ring. This result indicates that the shape of the collection probe could significantly influence the magnitude of the wall losses in the transition region.

For standard impactors it has been found useful to show the characteristic impaction curves with the abscissa expressed in units of the square root of the Stokes number, $\sqrt{St}$, which is a dimensionless particle size.[10] The Stokes number, as defined by Fuchs,[14] is the ratio of the particle stopping distance to the radius of the impactor throat,

$$St = \frac{\rho \quad C \ V_0 \ Dp^2/18\mu}{D_0/2} , \qquad (3)$$

where ρ_p is the particle density, C is the Cunningham slip correction factor, V_0 is the mean velocity in the throat, D_p is the particle diameter, μ is the fluid viscosity, and D_0 is the diameter of the throat. When plotted in this fashion, it has been found that the impaction curves are only slowly varying functions of S/D, the Reynolds number, and T/D. (See Figure 1 for definitions and S and T.) A similar representation is useful for showing the collection curves for virtual impactors. Figure 5 shows E_m as a function of $\sqrt{St}$ for measurements for which Q_1/Q_0, S/D_0, D_1/D_0, and T/D_0 were held constant and D_0, D_p, and Q_0 were varied.

Two values of D_0 were used; 0.3048 and the standard 0.3912 cm. For a particular data set either Q_0 was varied and D_p kept constant, or D_p was varied and Q_0 kept constant. For the former, this corresponds to a variation in Reynolds number, Re, of a factor of 4. In general, all the data for D_0 = 0.3048 cm fall on a single curve, while those for D_0 = 0.3912 cm lie slightly above the curve. This small variation is almost entirely due to different finishes on the inside walls of the collection probes. The inside wall of the larger probe was polished and had a maximum collection of 0.20, whereas the other one had a rougher surface and had a maximum collection of 0.25. A typical collection curve for a standard impactor is also shown on the figure; it is significantly steeper.

The collection characteristics of virtual impactors as a function of S/D_0, D_1/D_0, and Q_1/Q_0 were determined. The variation with T/D was not determined. The analytical studies indicate that it should be small for T/D_0 values greater than one-half. Studies were not made of the variation in collection characteristics for wide ranges of Reynolds numbers, since the analytical studies indicate that to see a significant deviation, it would be necessary to go to very low values of the Reynolds number. Such measurements would have been quite interesting, but would have required a complete redesign of the experimental apparatus. Figure 6 shows the variation in the collection characteristics for 2 micrometer-sized particles as a function of S/D_0, with all other parameters fixed at those of the standard. This variation with S/D_0 is significantly greater than that seen for a standard impactor and is related to the divergence of the jet as S/D_0 increases. Figure 7 shows the variation in the collection characteristics for 2 and 10 micrometer-sized particles as a function of D_1/D_0. For the 2 micrometer-sized particles the collection on the walls of the probe significantly increased for D_1/D_0 greater than 1.6. Studies by Loo, et al.[4] with solids particles showed similar results and also indicated that a minimum occurs at about D_1/D_0 = 1.3. For the 10 micrometer-sized particles increased wall losses in the collection probe begin at D_1/D_0 greater than 1.4.

The ratio Q_1/Q_0 was also varied. Figure 8 shows the results for Q_1/Q_0 = 0.10. The transition region is moved to larger particle sizes. The peak of the collection-probe wall-losses curve stays at around 0.20. There is also a small amount collected on the underside of the acceleration nozzle and on the acceleration nozzle support structure. Figure 9 shows the results for $Q_1/Q_0 = 0.03$. The transition region is moved to even larger particle sizes. The peak of the collection-probe wall-losses curve increases to about 0.30. In order to parameterize these results it is convenient to use the effective minor flow collection efficiency, E_m', which was previously defined. Figure 10 shows E_m' versus $\sqrt{St}$ for various values of Q_1/Q_0. It is seen that over a significant portion of the transition region the data is fit by a straight line. The line may be characterized by specifying the value of $\sqrt{St}$ at $E_m' = 0.50$ and the rate of change of the line, R, which is defined as

$$R = \frac{\sqrt{St}_{E_m' = 0.80} - \sqrt{St}_{E_m' = 0.20}}{\sqrt{St}_{E_m' = 0.50}}, \qquad (4)$$

where the subscript on $\sqrt{St}$ indicates the value of E_m'. Figure 11 shows the variation of $\sqrt{St}_{E_m' = 0.50}$ versus Q_1/Q_0. R remained constant at a value of 0.65.

In addition to the measurements described above, a number of measurements were made to determine the effect of changing the shape of the collection probe. Figure 12 shows two different shapes of collection probes that were used: a disc with a hole in it and a tube with rounded inside edges. The collection characteristics for the disc were identical with those for the standard. The collection characteristics for the tube with rounded inside edges were significantly different. The collection-probe wall-losses curve had approximately the same shape as that for the standard, but the magnitude was decreased by about 35%. There was a corresponding change in the collection curve for the major flow, while the collection curve for the minor flow remained unchanged. This result indicates that by rounding the inside edges of the collection probe particles that would have been deposited near the top are now able to remain in the major flow. Loo and Cork[15] have optimized the geometrical parameters for a particular design and have been able to reduce the losses for liquid particles to less than 1% for all particle sizes up to 20 micrometers.

Measurements were also made of the minor flow collection efficiency with PSL aerosols. The results are shown in Figure 13. Also shown on the figure are the curves for minor flow and receiving tube collection with DOP aerosols. Note that the results are quite similar for values of $\sqrt{St}$ less than 0.5, but the

DOP values are lower than the PSL values over the range from 0.5 to 0.9. The differences are explained by the fact that a droplet on striking a wall will stick, whereas a PSL sphere has a certain probability for rebounding. Apparently, the spheres that rebound from the walls can either enter the minor flow or be swept out of the tube in the major flow. The former appears to be much more likely for spheres with values of $\sqrt{St}$ near 0.8, while the latter for those with values less than 0.5. Loo, et al.[4] found that with solid aerosols of uranine the maximum collection in the receiving tube with this geometry was only a few percent

CONCLUSIONS

The purpose of this study was twofold: 1) to provide data that is useful in designing systems which employ virtual impactors, and 2) to develop an improved understanding of the principles of operation of virtual impactors. It was found that it is possible to parameterize much of the data by the introduction of the Stokes number and an effective minor flow collection efficiency. For given Q_1/Q_0, D_1/D_0, and S/D_0, there is a single curve which represents the minor flow collection efficiency as a function of $\sqrt{St}$. Analytical studies indicate that the curve should apply to quite low values of Reynolds number.[11] For different values of Q_1/Q_0, E_m' versus $\sqrt{St}$ is rather well-represented by a straight line whose rate of change stays constant and for which $\sqrt{St}_{E_m' = 0.50}$ is a smoothly decreasing function of Q_1/Q_0. Thus, Figures 10 and 11 can be used to determine effective minor flow collection efficiency curves for a wide range of system parameters. The study also indicated that the collection efficiencies for virtual impactors are more dependent on S/D_0 for values greater than one, than the collection efficiency for a standard impactor.

One disadvantage of the virtual impactor is that in the transition region particles are collected on the inside walls of the collection probe near the probe tip. It was found in this study and in the the study by Loo, et al.[4] that this collection is minimized if D_1/D_0 is kept at a value of about 1.3. Furthermore, the amount that is collected is a sensitive function of the probe geometry.

Rounding the inside of the probe tip, polishing this surface, and maintaining good alignment between the acceleration nozzle and collection probe minimizes the amount collected. Using trial-and-error methods, Loo and Cork[15] have been able to minimize the collection peak to less than 1% for a particular set of flow and geometry conditions. At this time it is not known whether such dramatic improvements are possible for arbitrary flow conditions.

REFERENCES

1. Hounam, R. F., and R. J. Sherwood. The Cascade Centripeter: A Device for Determining the Concentration and Size Distribution of Aerosols. Ind. Hyg. J., 26:122-131, 1965.

2. Conner, W. D. An Inertial-Type Particle Separator for Collecting Large Samples. J. Air Pollut. Contr. Assoc., 16(1):35-38, 1966.

3. Dzubay, T. G., and R. K. Stevens. Ambient Air Analysis with Dichotomous Sampler and X-ray Fluorescence Spectrometer. Environ. Sci. Technol., 9(7): 663-668, 1975.

4. Loo, B. W., J. M. Jaklevic, and F. S. Goulding. Dichotomous Virtual Impactors for Large-Scale Monitoring of Airborne Particulate Matter. In: Fine Particles: Aerosol Generation, Measurement, Sampling and Analysis, B. Y. H. Liu, ed. Academic Press, New York, 1976. pp. 311-350.

5. Loo, B. W., R. S. Adachi, C. P. Cork, F. S. Goulding, J. M. Jaklevic, D. A. Landis, and W. L. Searles. A Second Generation Dichotomous Sampler for Large-Scale Monitoring of Airborne Particulate Matter. Lawrence Berkeley Laboratory Report LBL-8725, 1979.

6. McFarland, A. R., R. W. Bertch, G. L. Fisher, and B. A. Prentice. Fractionator for Size Classification of Aerosolized Solid Particulate Matter. Environ. Sci. Technol., 11(8):781-784, 197.

7. Kotrappa, P., D. P. Bhanti, S. K. Dua, and P. P. Joshi. A Single Stage Centripeter for Rapid Analysis of Long-Lived Alpha Emitters in Air. Health Physics, 27:103-108, 1974.

8. Yule, T. J. An On-Line Monitor for Alpha-Emitting Aerosols. IEEE Trans. Nuc. Sci., NS-25(1):762-766, 1978.

9. McFarland, A. R., C. A. Ortiz, and R. W. Bertch, Jr. Particle Collection Characteristics of a Single-Stage Dichotomous Sampler. Environ. Sci. Technol., 12(6):679-682, 1978.

10. Marple, V. A., and B. Y. H. Liu. Characteristics of Laminar Jet Impactors. Environ. Sci. Technol., 8(7):648-654, 1974.

11. Marple, V. A. and C. M. Chien. A Theoretical Study of Virtual Impactors. Part. Tech. Lab. Publication 378, University of Minnesota, 1978. Submitted to Environ. Sci. Technol.

12. Hassan, Y. A., B. G. Jones, and T. J. Yule. An Analytical Study of Virtual Impactor Aerosol Separators. To be published in Trans. Am. Nuc. Soc., San Francisco Meeting, 1979.

13. Marple, V. A., N. J. Barsic, and K. T. Whitby. Instruments and Techniques for Dynamic Particle Size Measurements of Coal Dust. Part. Tech. Lab. Publication 215, University of Minnesota, 1974.

14. Fuchs, N. A. The Mechanics of Aerosols, Pergamon Press, New York, 1964.

15. Loo, B. W., and C. P. Cork. High-Efficiency Virtual Impactors. Submitted to Environ. Sci. Technol.

FIGURE CAPTIONS

Figure 1. Schematic view of a virtual impactor showing representative streamlines and particle trajectories.

Figure 2. Apparatus for measuring the collection characteristics of virtual impactors. Some of the key components are indicated: 1) acceleration nozzle, 2) flow transition cone, and 3) collection probe.

Figure 3. Collection efficiencies for the standard virtual impactor.

Figure 4. Modified collection probe with annular inserts.

Figure 5. Minor flow collection efficiencies for virtual impactors having $Q_1/Q_0 = 0.25$, $S/D_0 = 1.0$, and $D_1/D_0 = 1.28$, and for which D_0, Q_0, and D_p were varied. The dashed curve shows the collection efficiency for a well-designed standard impactor.

Figure 6. Variation in the collection efficiencies for 2 micrometer-sized particles as a function of S/D_0.

Figure 7. Variation in the collection efficiencies for 2 and 10 micrometer-sized particles as a function of D_1/D_0.

Figure 8. Collection efficiencies for a virtual impactor for which all the parameters are the same as those for the standard except $Q_1/Q_0 = 0.10$.

Figure 9. Collection efficiencies for a virtual impactor for which all the parameters are the same as those for the standard except $Q_1/Q_0 = 0.03$.

Figure 10. Effective minor flow collection efficiencies for various values of Q_1/Q_0.

Figure 11. The variation in $\sqrt{St}$ at which the effective minor flow collection efficiency is 0.50 as a function of Q_1/Q_0.

Figure 12. Modified collection probes.

Figure 13. Collection efficiencies for virtual impactors for which $Q_1/Q_0 = 0.25$, $S/D_0 = 1.0$, and $D_1/D_0 = 1.28$ for PSL and DOP aerosols.

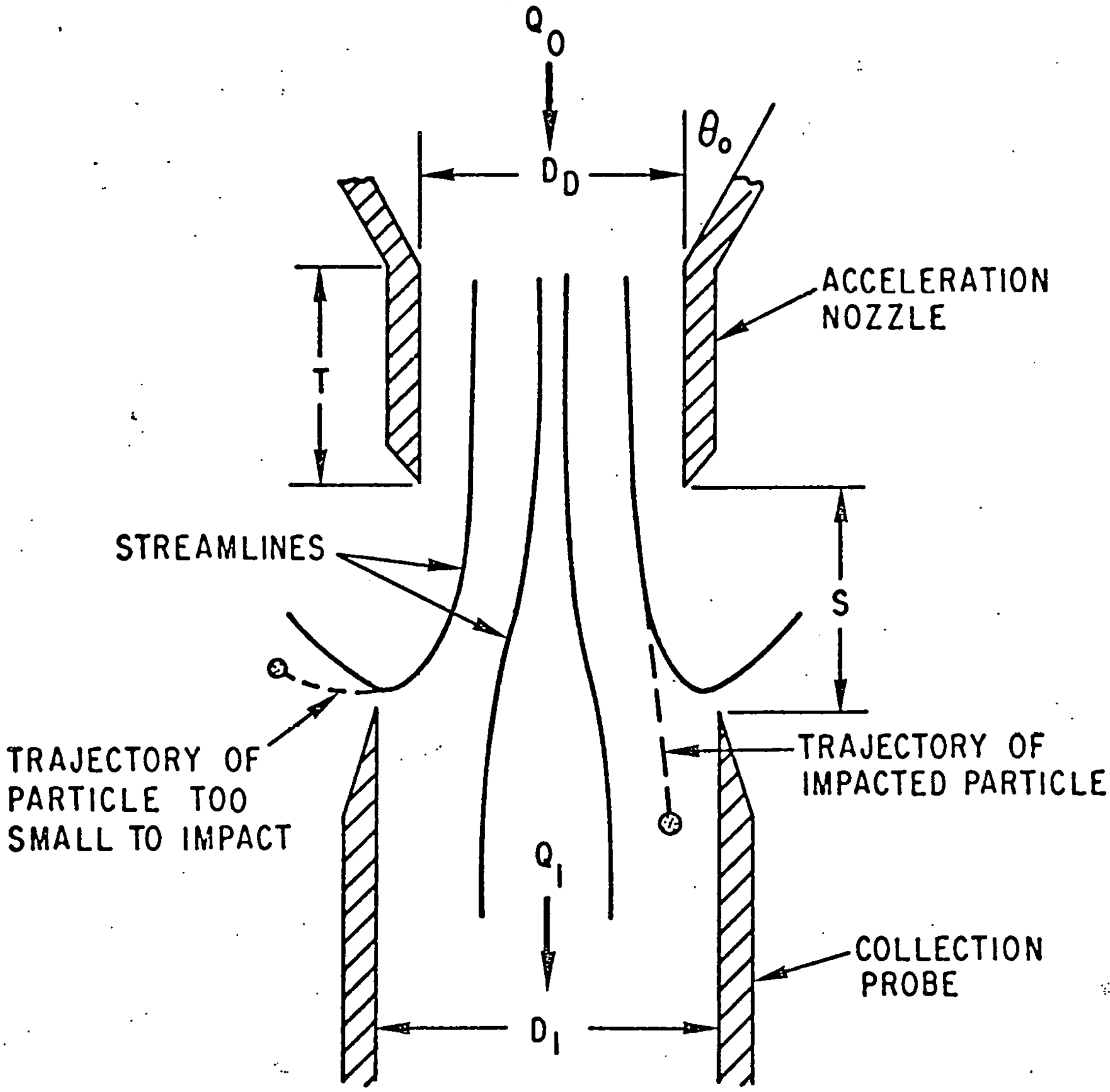

Figure 1. Schematic view of a virtual impactor showing representative streamlines and particle trajectories.

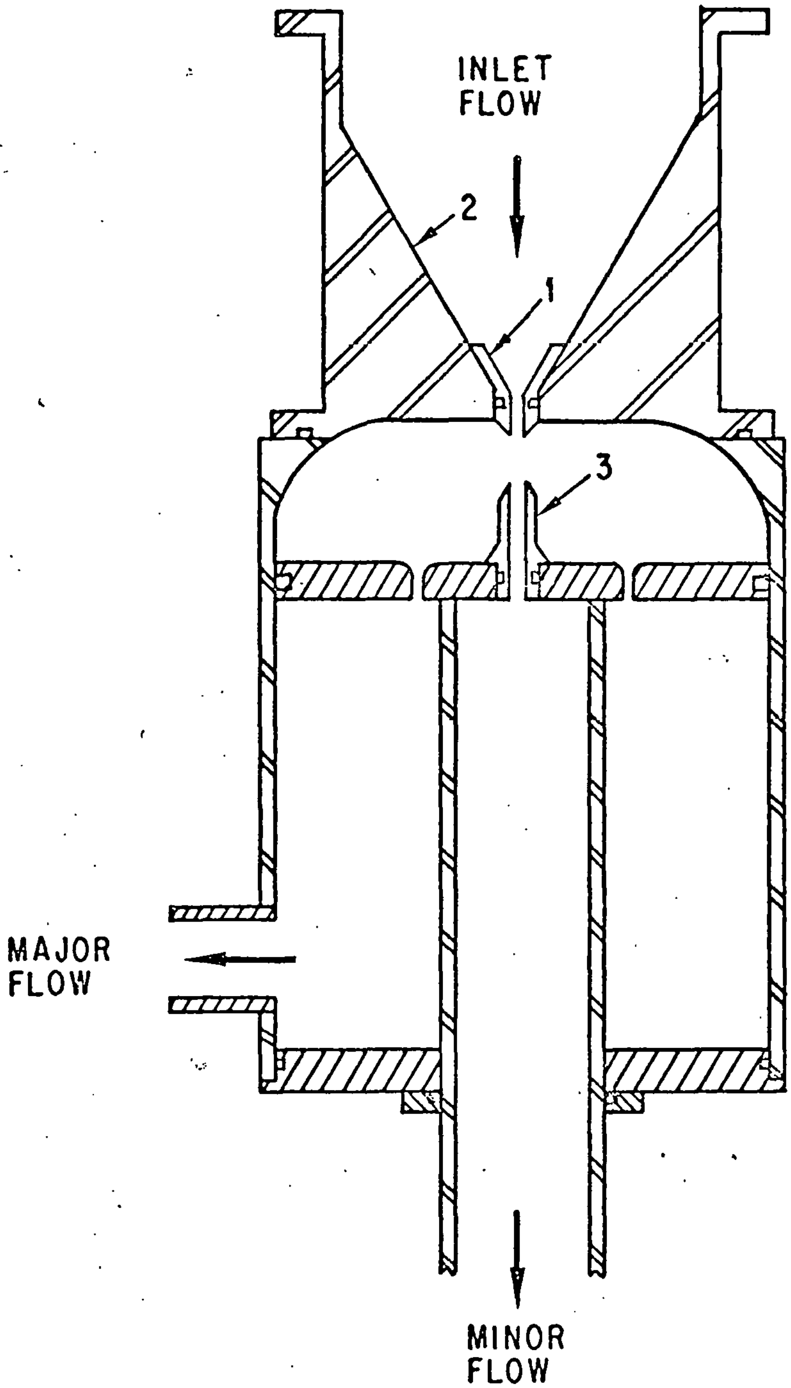

Figure 2. Apparatus for measuring the collection characteristics of virtual impactors. Some of the key components are indicated: 1) acceleration nozzle, 2) flow transition cone, and 3) collection probe.

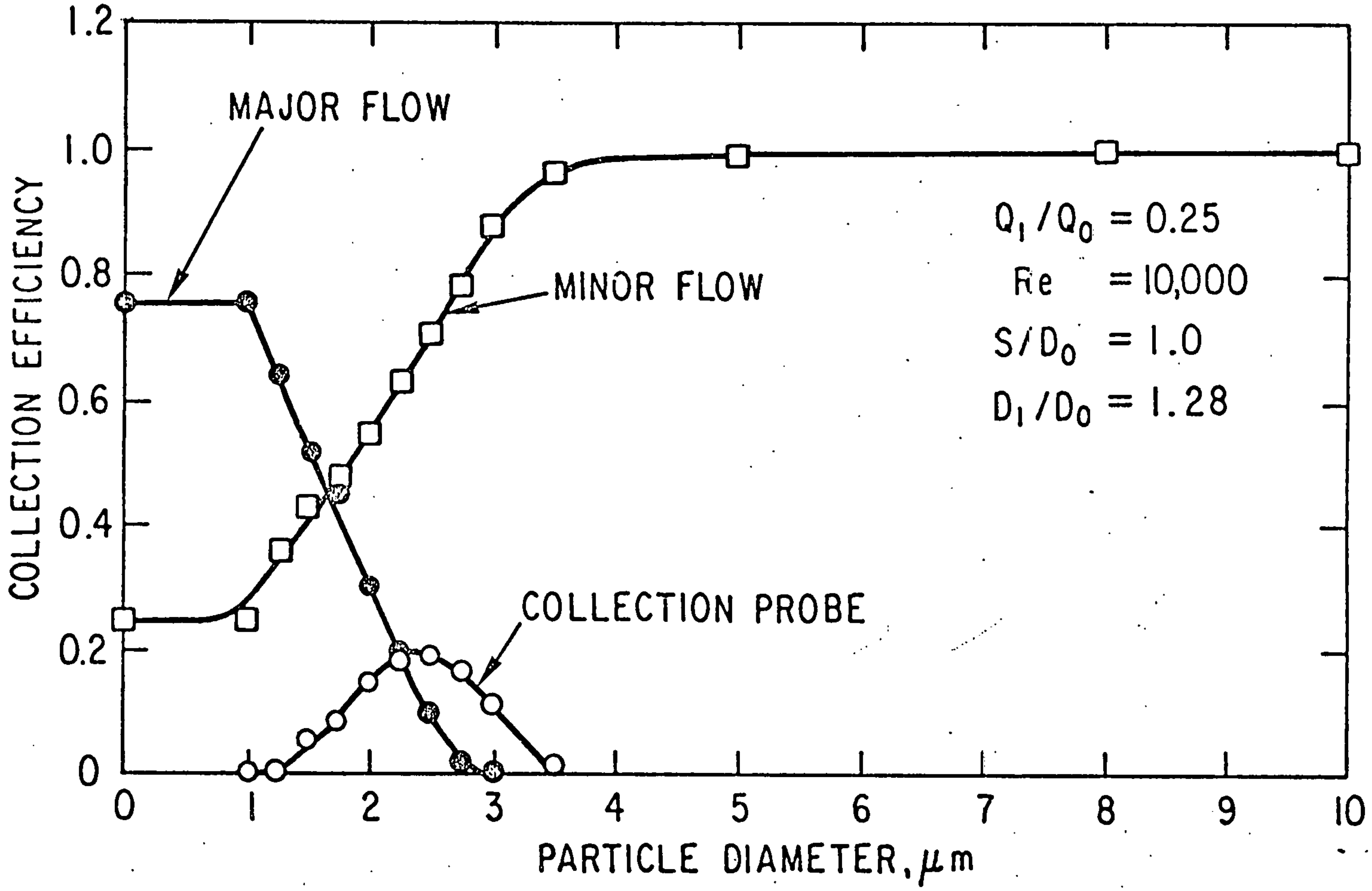

Figure 3. Collection efficiencies for the standard virtual impactor.

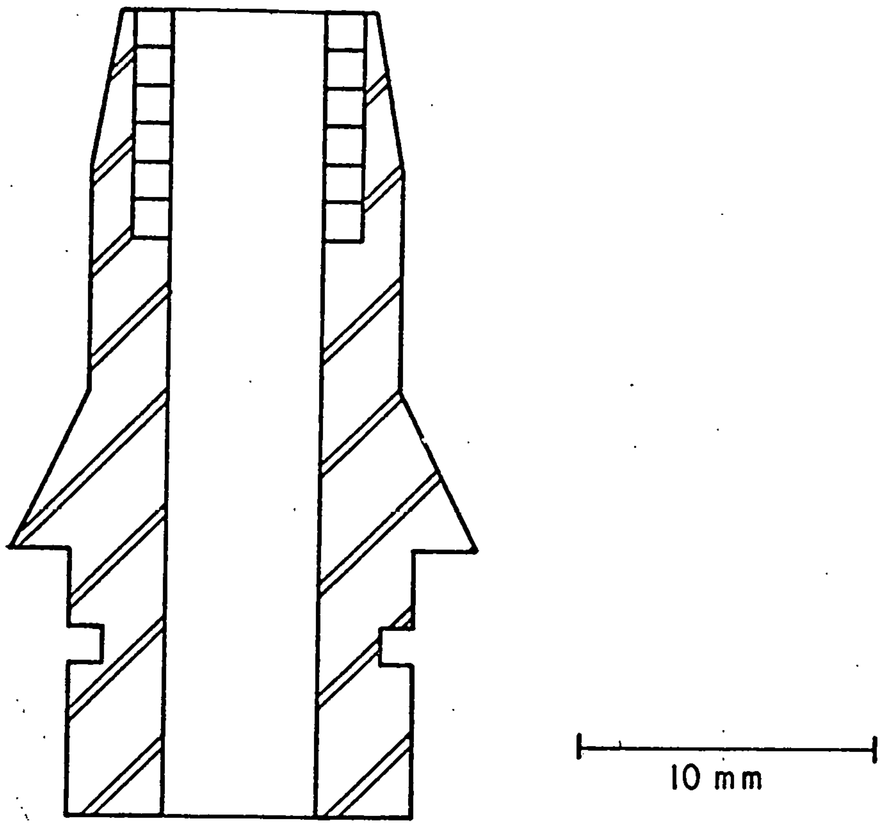

Figure 4. Modified collection probe with annular inserts.

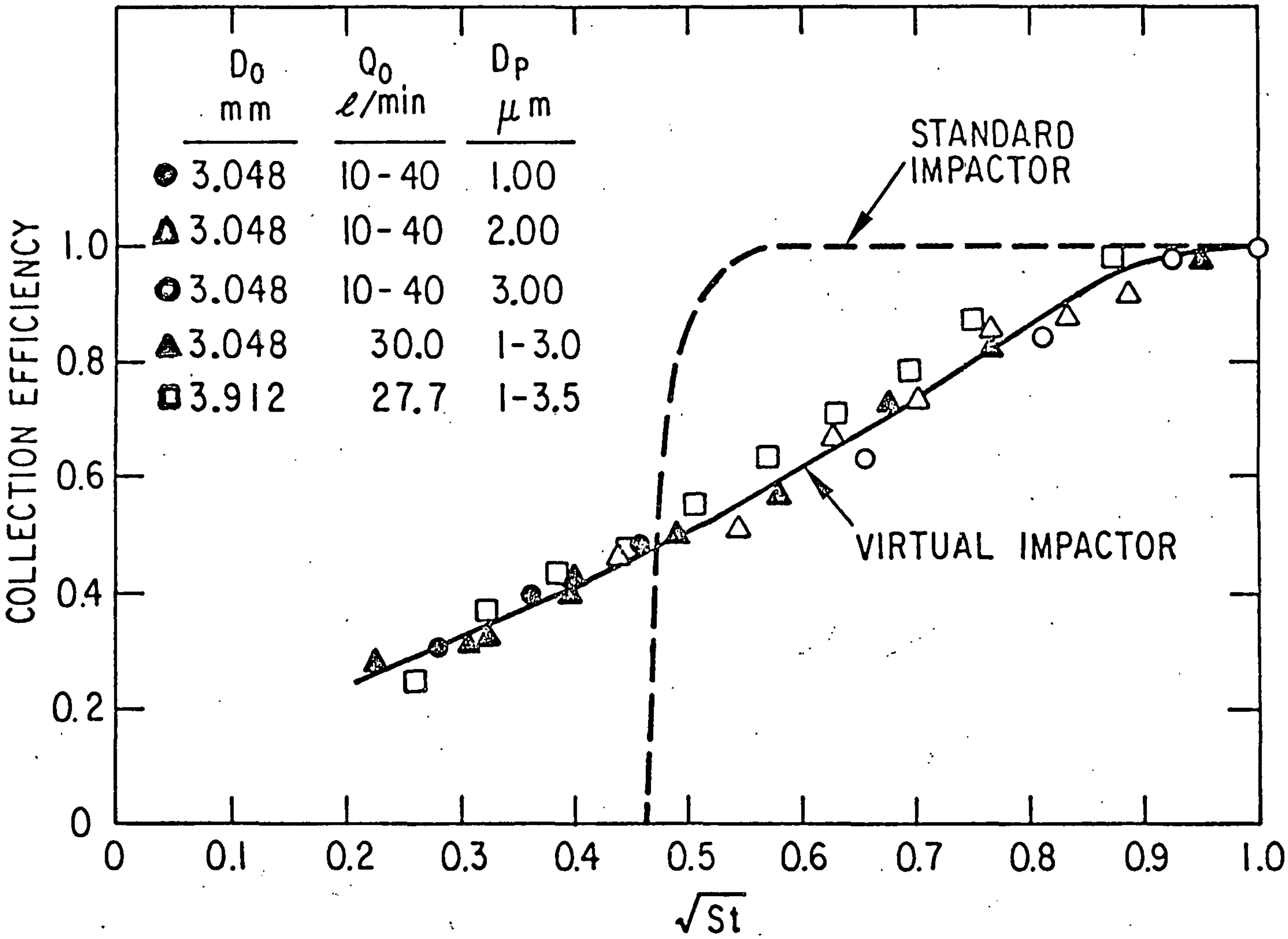

Figure 5. Minor flow collection efficiencies for virtual impactors having $Q_1/Q_0 = 0.25$, $S/D_0 = 1.0$, and $D_1/D_0 = 1.28$, and for which D_0, Q_0, and D_p were varied. The dashed curve shows the collection efficiency for a well-designed standard impactor.

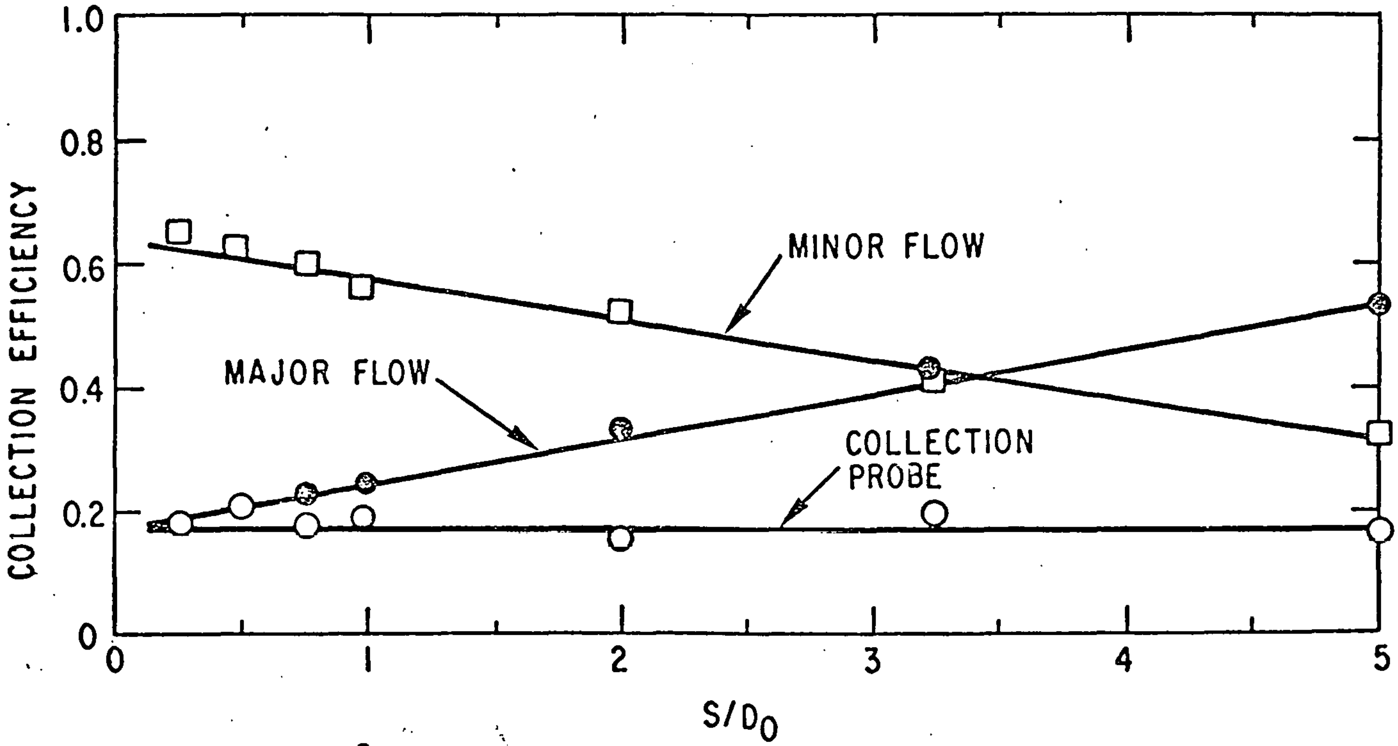

Figure 6. Variation in the collection efficiencies for 2 micrometer-sized particles as a function of S/D_0.

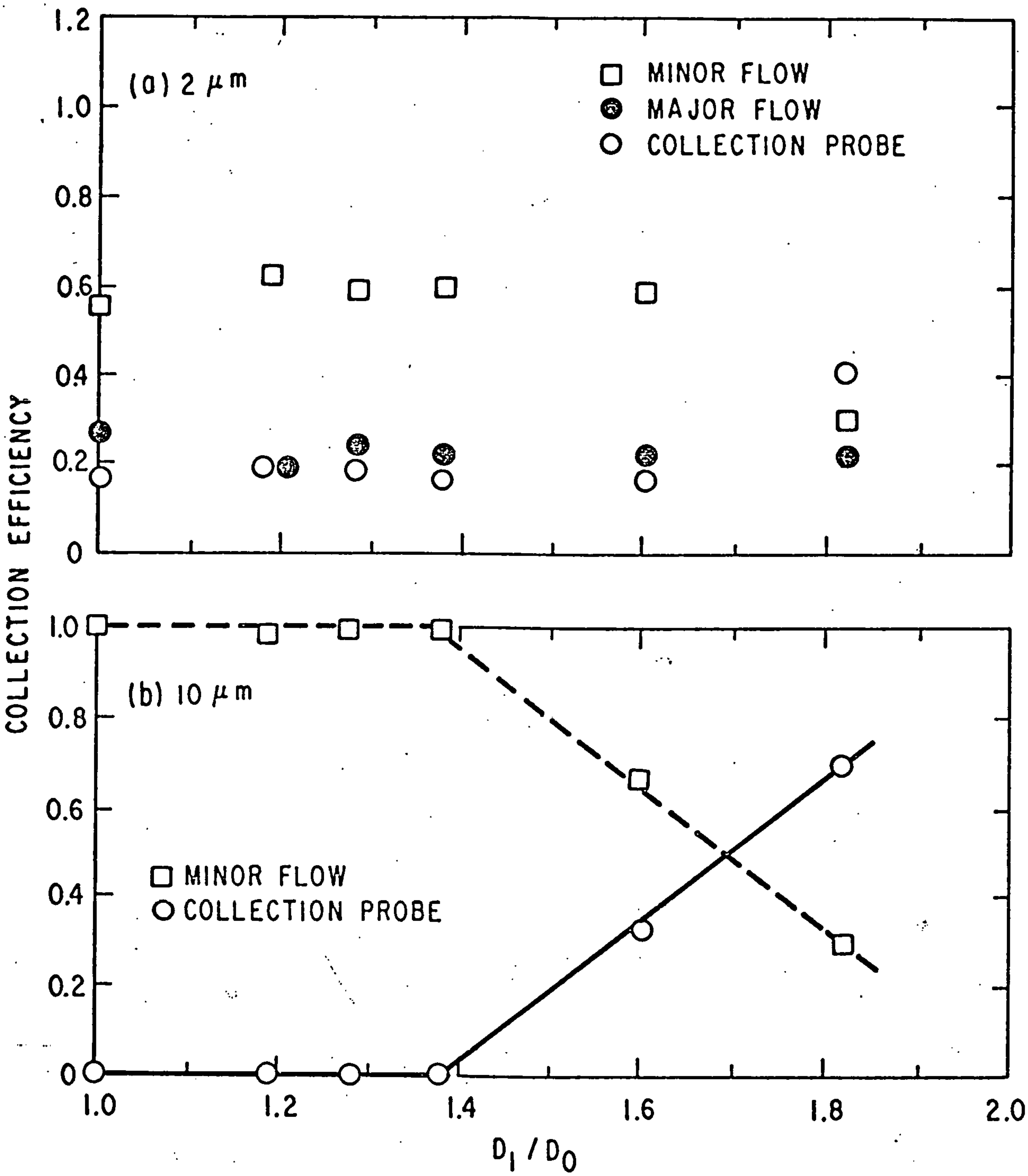

Figure 7. Variation in the collection efficiencies for 2 and 10 micrometer-sized particles as a function of D_1/D_0.

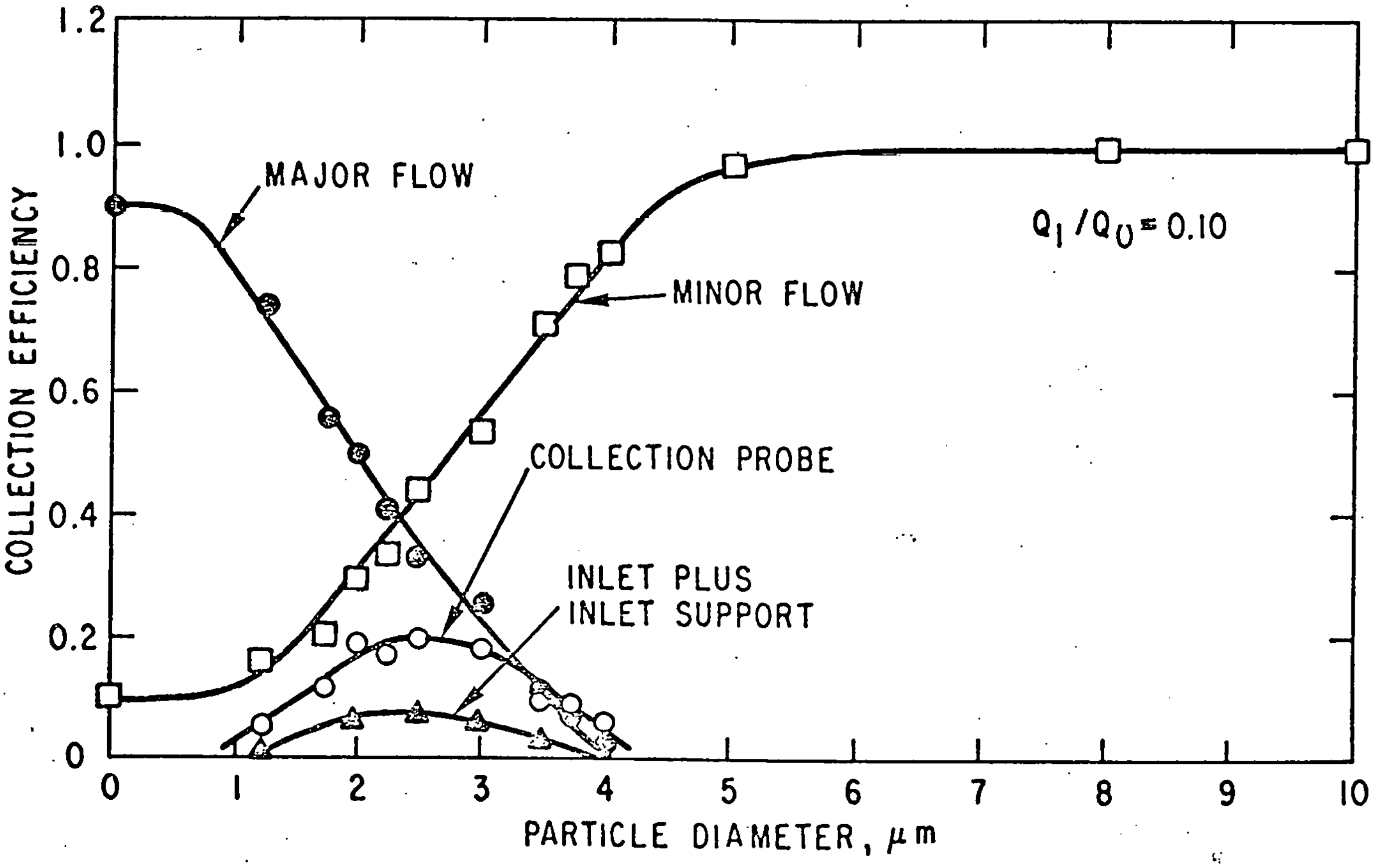

Figure 8. Collection efficiencies for a virtual impactor for which all the parameters are the same as those for the standard except $Q_1/Q_0 = 0.10$.

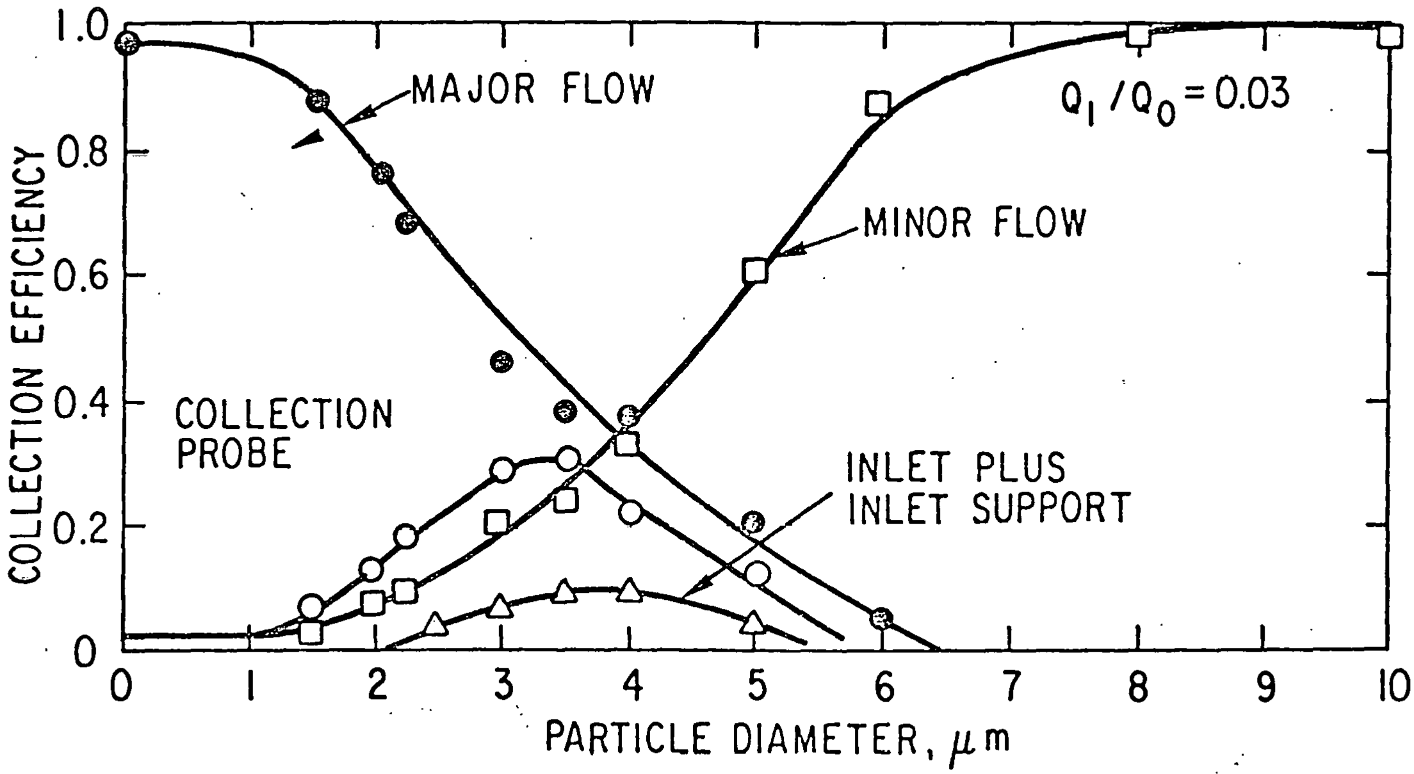

Figure 9. Collection efficiencies for a virtual impactor for which all the parameters are the same as those for the standard except $Q_1/Q_0 = 0.03$.

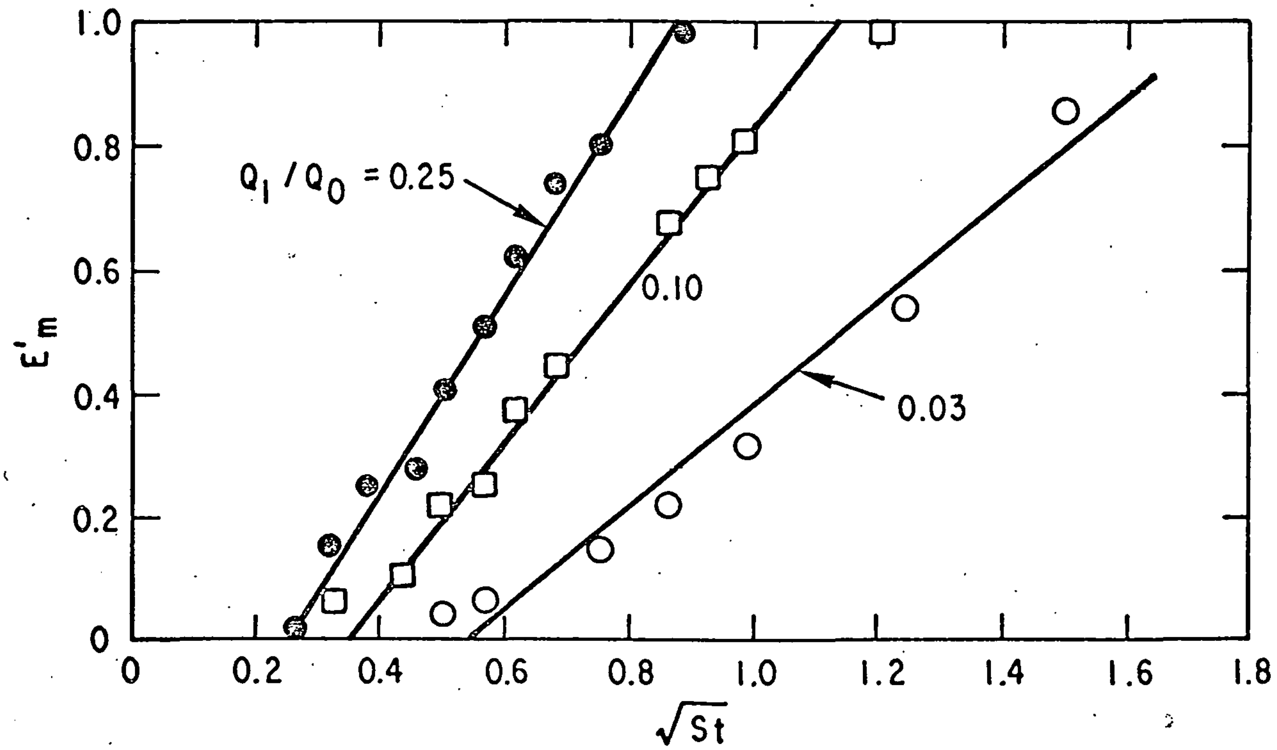

Figure 10. Effective minor flow collection efficiencies for various values of Q_1/Q_0.

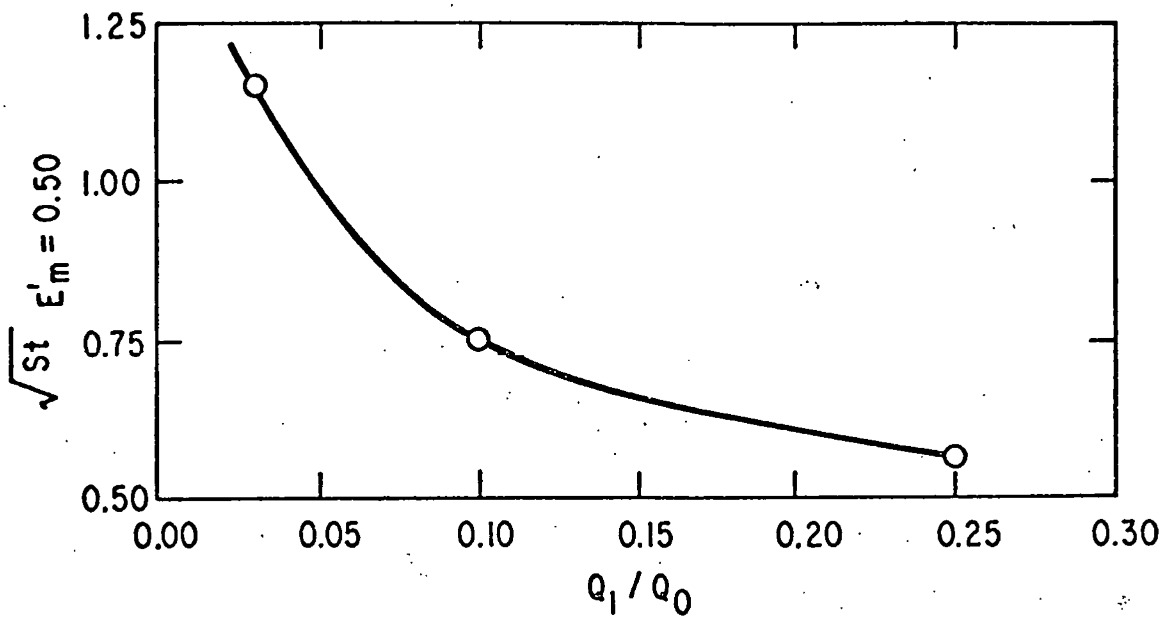

Figure 11. The variation in $\sqrt{St}$ at which the effective minor flow collection efficiency is 0.50 as a function of Q_1/Q_0.

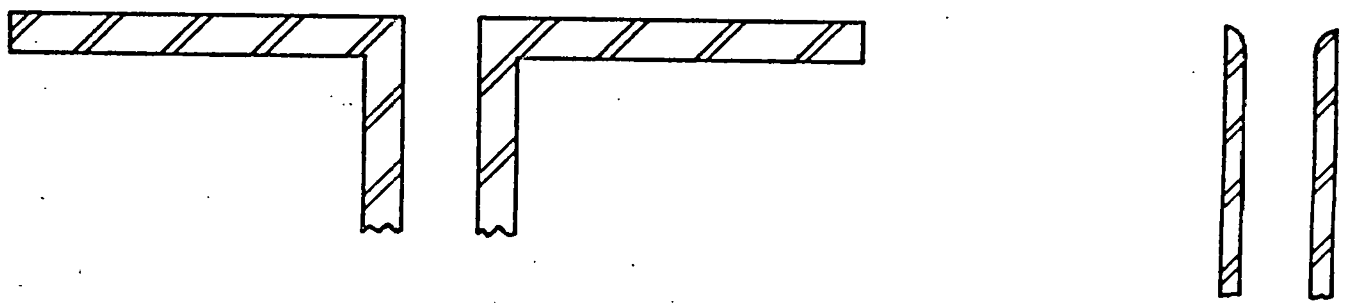

(a) DISC WITH A HOLE THROUGH IT. (b) TUBE WITH ROUNDED INSIDE EDGES

Figure 12. Modified collection probes.

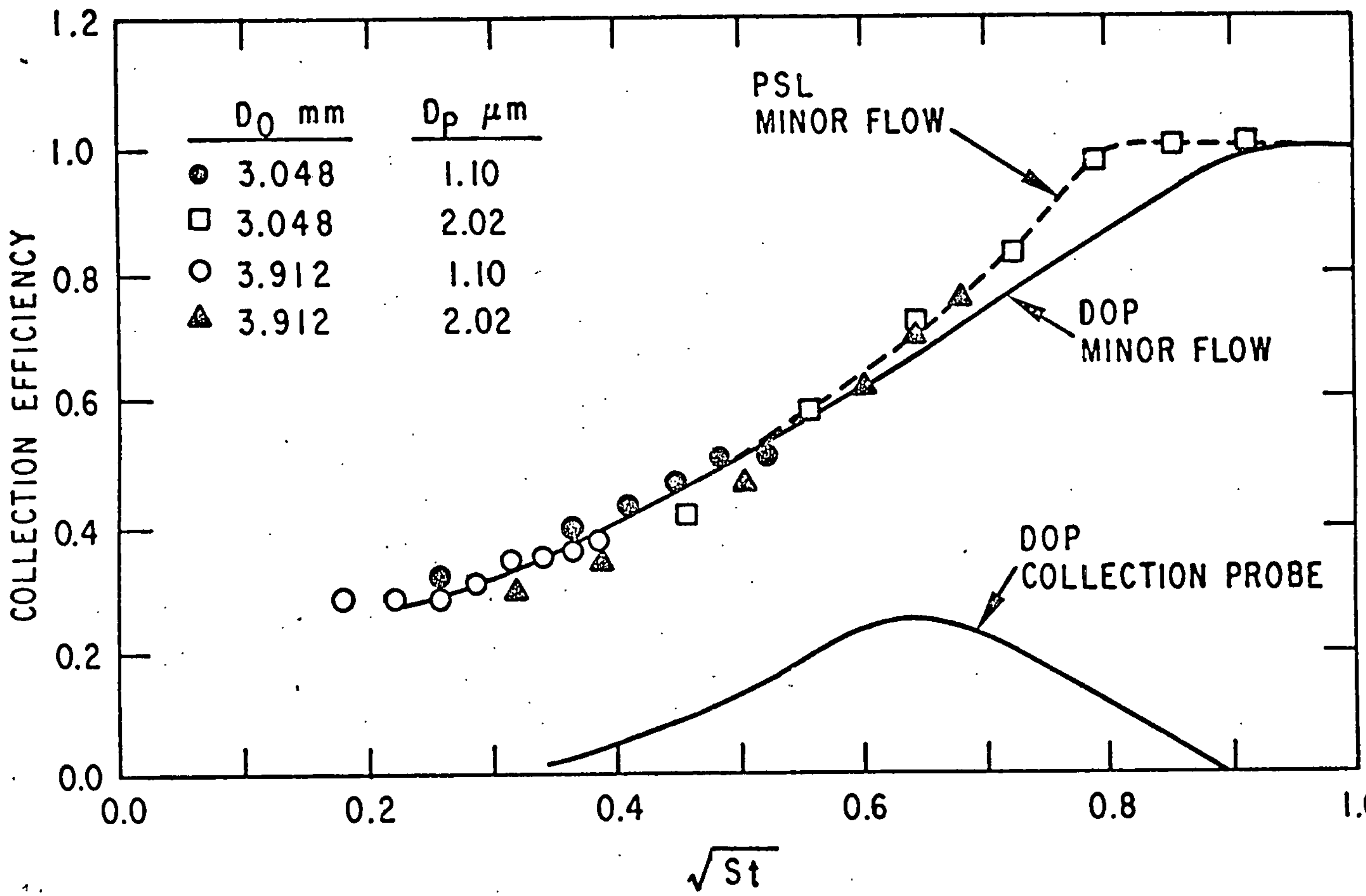

Figure 13. Collection efficiencies for virtual impactors for which $Q_1/Q_0 = 0.25$, $S/D_0 = 1.0$, and $D_1/D_0 = 1.28$ for PSL and DOP aerosols.

TABLE 1. GEOMETRICAL AND FLOW PARAMETERS FOR THE STANDARD VIRTUAL IMPACTOR

Parameter	Value
D_0	3.912 mm
D_1/D_0	1.28
S/D_0	1.0
T/D_0	2.0
Q_0	27.7 l/min[a]
Q_1/Q_0	0.25

[a]Corresponds to a jet Reynolds number of 10,000.